SIMULATION EXPERIMENTS FOR GAMMA-RAY MAPPING OF PLANETARY SURFACES: SCATTERING OF HIGH-ENERGY NEUTRONS. J. Brückner[1], P. Englert[2], R. C. Reedy[3], and H. Wänke[1]. ([1]Max-Planck-Institut für Chemie, Mainz, FRG; [2]Institut für Kernchemie, Köln, FRG; [3]Los Alamos National Laboratory, Los Alamos, NM, USA)

The concentration and distribution of certain elements in surface layers of planetary objects specify constraints on models of their origin and evolution. This information can be obtained by means of remote sensing gamma-ray spectroscopy (1), as planned for a number of future space missions, i.e. Mars, Moon, asteroids, and comets.

The surface of a planetary body is bombarded by energetic particles of cosmic-rays, which produce a cascade of secondary particles, such as neutrons. Nonelastic scattering and capture reactions of these neutrons play an important role in the production of discrete-energy gamma-ray lines which can be measured by a gamma-ray detector on board of an orbiter. This allows to determine the abundances of many elements, as O, Al, Si, K, Ca, Fe, Th, and U, in the upper 50 centimeters of a planet's surface layer.

To investigate the gamma-rays made by interactions of neutrons with matter, thin targets of different composition were placed between a neutron-source and a high-resolution germanium spectrometer. Gamma-rays in the range of 0.1 to 8 MeV were accumulated.

In one set of experiments (2) a 14-MeV neutron generator using the T(d,n) reaction as neutron-source was placed in a small room. Scattering in surrounding walls produced a spectrum of neutron energies from 14 MeV down to thermal. This complex neutron-source induced mainly neutron-capture lines and only a few scattering lines. As a result of the set-up, there was a considerable background of discrete lines from surrounding material. A similar situation exists under planetary exploration conditions: gamma-rays are induced in the planetary surface as well as in the spacecraft.

To investigate the contribution of neutrons with higher energies, an experiment for the measurement of prompt gamma radiation was set up at the end of a beam-line of the isochronous cyclotron of the KFA Jülich, FRG (cf. fig. 1). Energetic neutrons were produced by bombardement of a 1 cm thick

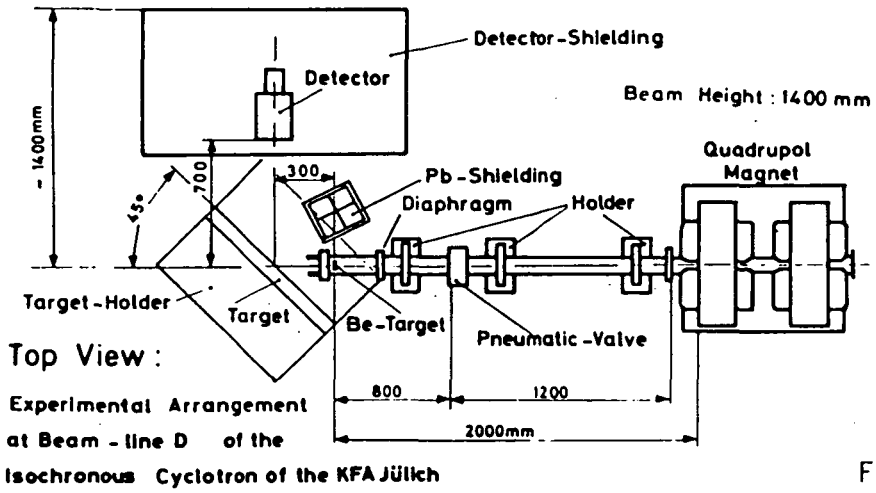

Fig. 1

SIMULATION EXPERIMENTS FOR GAMMA-RAY MAPPING
Brückner, J. et al.

Be-target with deuterons of energies of 45, 60, and 78 MeV, resulting in maximal neutron energies of 22.5, 30, and 39 MeV respectively. Typical deuteron-beam currents varied between 200 and 600 pA depending on the target material exposed to them. The majority of the neutrons produced by the Be(d,n) reaction is emitted in forward direction and hits the extended targets positioned at an angle of 45° to the beam axis.

Gamma-rays were measured with a 92-cm^3 high purity germanium-detector located at an angle of 90° to the beam axis and 70 cm away from the geometric center of the target-plates. The front side of the detector was shielded by a 2 cm plate made of borated polyethylene. The other sides were consecutively surrounded by lead, boron, and paraffin in order to shield it from background gamma radiation and scattered neutrons. Gamma radiation from the Be-target and its direct environment was suppressed by an additional 20-cm lead shield.

During in-beam operation, the germanium-detector had a resolution of about 6 keV at 7 MeV. The detector signals were processed by conventional amplifiers and ADCs, and stored in 8000 channels of two combined multichannel analyzers.

The gamma-ray spectra were unfolded by an interactive computer program using a modified Gauss-Newton algorithm. A large gamma-ray library provided data for the identification of the source-reactions.

Several correction factors had to be applied to the measured line intensities: i) the total neutron-flux factor was determined by using peaks of suitable reactions in the spectrum itself; ii) the background correction was determined by comparing the gamma-ray emission of targets of different composition; iii) the absolute efficiency was determined by using radioactive standards for the low energy range and by an iron-target for the high-energy range; iv) the mass attenuation coefficient of the detector shielding-material was determined experimentally and the energy dependent absorption factor of the gamma-rays was calculated; v) the gamma selfabsorption factor of the three-dimensional target was calculated by using the appropriate mass attenuation coefficients.

Several targets were irradiated with neutrons of different energies. In contrast to the 14-MeV experiments, the capture lines are very week and result mainly from the surrounding material. The scattering and (n,2n) reaction gamma-rays dominate the spectra (cf. Fe-spectrum in fig. 2).

The gamma-ray lines of e.g. iron and their measured intensities, considering all necessary corrections, are listed in table 1. It can be seen, that the intensities for 30 and 39-MeV neutrons are very similar in most cases. For 22.5-MeV neutrons increased intensities are found for almost all energies. This is a result of the general decrease of the cross sections with increasing energy in the energy interval under question. Compared to 14-MeV, four more lines were observed in the 22.5 and 30-MeV experiments: 1038, 2113, 2523, and 3601 keV. 39-MeV neutrons revealed an additional scattering line at 2601 keV.

Combining the results of the 14-MeV and the 'high-energy' experiments we get a rather realistic simulation of the expected gamma-flux from planetary surfaces. The complexity of the accumulated gamma-ray spectra illustrates what a gamma-ray experiment may encounter during a mission.

Ref.: (1) R. C. Reedy (1978) Proc. Lunar Planet. Sci. Conf. 9th, p. 2961
(2) J. Brückner, R. C. Reedy, and H. Wänke (1984) Lunar Plan. Sci. XV, p.98

GAMMA-ENERGY [keV]	SOURCE-REACTION	NEUTRON ENERGY 22.5 MeV	30 MeV	39 MeV
846.7	Fe(n,ng)	$1.51 \cdot 10^{8}$	$9.65 \cdot 10^{7}$	$9.81 \cdot 10^{7}$
931.2	Fe(n,2ng)	$9.17 \cdot 10^{6}$	$9.43 \cdot 10^{6}$	$1.01 \cdot 10^{7}$
1038.0	Fe(n,ng)	$8.17 \cdot 10^{6}$	$6.78 \cdot 10^{6}$	$6.82 \cdot 10^{6}$
1238.3	Fe(n,ng)	$3.36 \cdot 10^{7}$	$2.42 \cdot 10^{7}$	$2.33 \cdot 10^{7}$
1316.4	Fe(n,2ng)	$7.05 \cdot 10^{6}$	$8.56 \cdot 10^{6}$	$9.11 \cdot 10^{6}$
1407.7	Fe(n,ng)	$7.77 \cdot 10^{6}$	$8.33 \cdot 10^{6}$	$1.16 \cdot 10^{7}$
1810.9	Fe(n,ng)	$1.83 \cdot 10^{7}$	$9.23 \cdot 10^{6}$	$1.01 \cdot 10^{7}$
2112.9	Fe(n,ng)	$9.60 \cdot 10^{6}$	$4.02 \cdot 10^{6}$	$4.41 \cdot 10^{6}$
2523.1	Fe(n,ng)	$4.39 \cdot 10^{6}$	$2.62 \cdot 10^{6}$	$2.80 \cdot 10^{6}$
2601.0	Fe(n,ng)	n.d.	n.d.	$7.28 \cdot 10^{5}$
3601.9	Fe(n,ng)	$9.69 \cdot 10^{5}$	$2.20 \cdot 10^{6}$	$1.45 \cdot 10^{6}$

Table 1. Measured and corrected intensities [dpm] of iron gamma-rays for different neutron energies (n.d. = not determined).

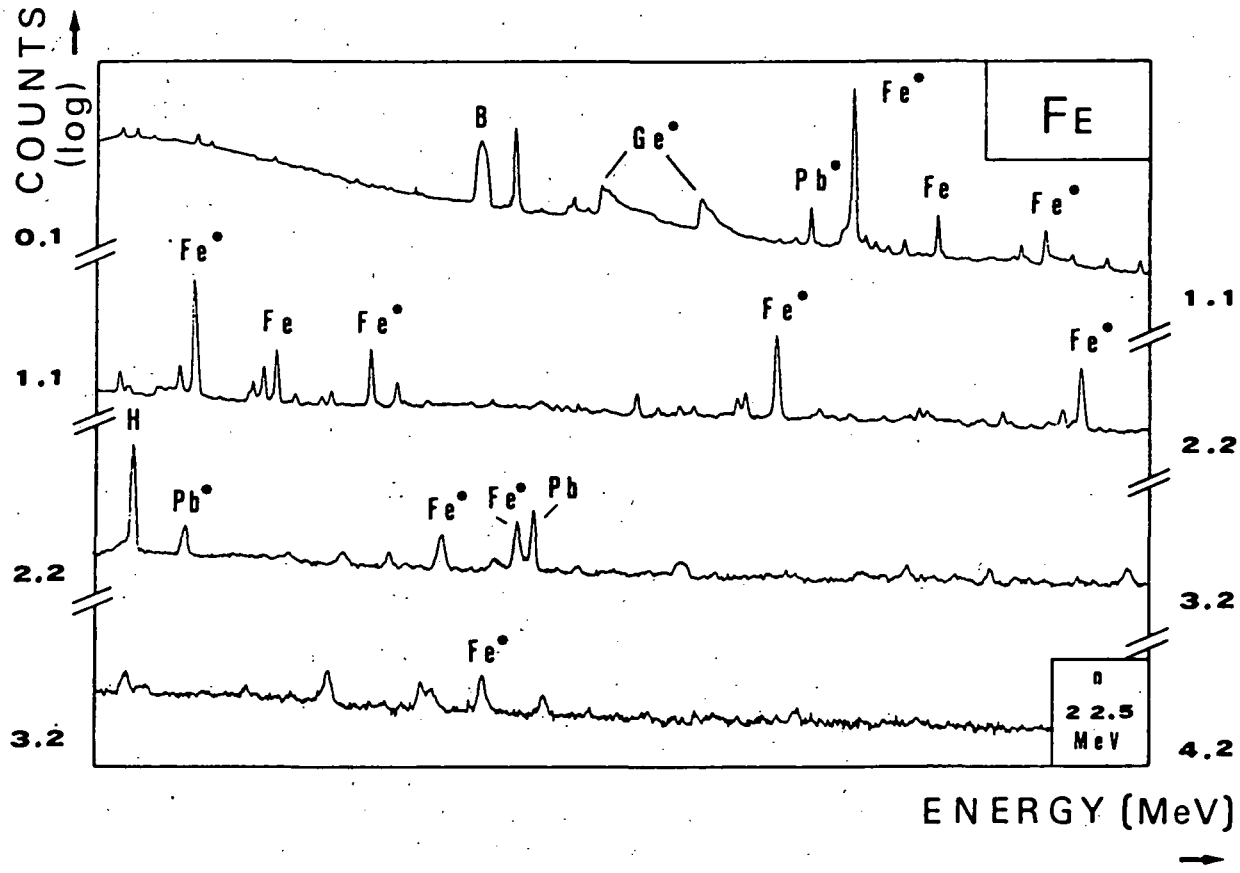

Fig. 2 Low energy part of in-beam gamma-ray spectrum of iron and surrounding material, induced by 22.5 MeV neutrons (* = (n,nγ)).